

# Separation of Bulk Hydrogen Sulfide–Hydrogen Mixtures by Selective Surface Flow Membrane

D. J. Parrillo, C. Thaeron, and S. Sircar  
Air Products and Chemicals, Inc., Allentown, PA 18195

*The separation performance of binary hydrogen sulfide–hydrogen mixtures by a nanoporous carbon membrane called selective surface flow (SSF) membrane is described. The membrane selectively permeates  $H_2S$  from  $H_2$ , and a  $H_2$ -enriched stream is produced at the feed-gas pressure. A two-stage embodiment of the SSF membrane is described for production of high-purity  $H_2$  with high  $H_2$  recovery from an equimolar  $H_2S$ - $H_2$  feed gas. A novel protocol for operation of the two-stage membrane is needed to achieve that separation goal.*

## Introduction

A nanoporous carbon membrane called Selective Surface Flow (SSF) membrane has been developed by Air Products and Chemicals, Inc. (Rao et al., 1992; Rao and Sircar, 1993). It consists of a thin layer (2–3  $\mu\text{m}$ ) of a nanoporous (6–7 Å pore diameter) carbon matrix supported on a macroporous (<1- $\mu\text{m}$  pore diameter) tubular alumina support. The pore-size distribution of the membrane was very narrow as shown by  $\text{CH}_4$  diffusivity measurements (Rao and Sircar, 1996). It is produced by coating the bore size of the tubular support with a polyvinylidene chloride latex film and then carbonizing the polymer by heating in an inert atmosphere. Only one coat of the polymer and a single heating step are used. The details of the carbonizing conditions and pore characteristics of the membrane are given elsewhere (Rao et al., 1992; Rao and Sircar, 1993, 1996; Anand et al., 1997). The pores of the alumina support are much larger than the pores of the carbon layer, and thus the support pores do not influence the separation characteristics of the SSF membrane.

The membrane separates gas mixtures by an adsorption–surface diffusion–desorption mechanism (Rao and Sircar, 1993). The gas mixture to be separated is passed through the bore side of the membrane at a superambient pressure level ( $P^H$ ) while keeping the permeate side at a near-ambient pressure level ( $P^L$ ). Certain components of the feed-gas mixture are selectively adsorbed on the pore walls of the carbon membrane, followed by their selective surface diffusion on the pore walls to the low-pressure side where they are desorbed into the permeate gas phase. Consequently, the mem-

brane produces a gas stream enriched in the less selectively adsorbed components of the feed-gas mixture as the high-pressure effluent gas, while a gas stream enriched in the more selectively adsorbed components of the feed gas is produced as the low pressure effluent gas. This is often very desirable because the less selectively adsorbed components form the desired product gas in many practical applications.

Adsorbates having larger molecular size, higher polarizability, and larger permanent polarity are selectively adsorbed on the membrane walls and they selectively permeate through the membrane. This is in contrast with the characteristics of most polymeric membranes where the smaller molecules of a gas mixture preferentially permeate through the membranes by a solution–diffusion mechanism. The separation mechanism of the SSF membrane provides high permeance with high permselectivities of the adsorbed components while requiring relatively low feed-gas pressures (0.24–1.5 MPa). Typical polymeric membranes, on the other hand, exhibit a reciprocal relationship between permeance and permselectivity of the permeated gas, and they require relatively larger feed-gas pressures (> 1.5 MPa) for practical operation. These advantages of the SSF membrane have led to many separation concepts of practical interest, such as hydrogen recovery from refinery and chemical-waste gases and fractionation of hydrocarbon mixtures (Rao et al., 1995; Anand et al., 1995).

The purpose of the present work is to report on the separation characteristics of bulk  $H_2S$ - $H_2$  mixtures under various operating conditions using the SSF membrane and to describe a novel mode of operation of the membrane system for enhancing the  $H_2S$ - $H_2$  separation.

Correspondence concerning this article should be addressed to S. Sircar.

Hydrogen sulfide is selectively adsorbed and permeated through the SSF membrane because (a) it has a large permanent dipole moment ( $0.97 \times 10^{-18}$  esu), while the hydrogen has a weak quadrupole moment ( $0.66 \times 10^{-26}$  esu  $\cdot$  cm<sup>2</sup>) (Stogryn and Stogryn, 1966; Weast et al., 1978), and (b) the polarizability of H<sub>2</sub>S ( $37.8 \times 10^{-25}$  cm<sup>3</sup>) is much larger than that of H<sub>2</sub> ( $7.9 \times 10^{-25}$  cm<sup>3</sup>) (Hirschfelder et al., 1954). The kinetic diameters of H<sub>2</sub>S and H<sub>2</sub> are, respectively, 3.60 and 2.92 Å (Breck, 1973).

## Experimental Methods and Data Analysis

Figure 1 is a diagram of the apparatus used for evaluating the separation performance of binary H<sub>2</sub>S-H<sub>2</sub> mixtures by the SSF membrane. A single tube of the SSF membrane (30 cm long, 0.56-cm internal diameter, 0.165-cm-thick support wall) was mounted in a cylindrical membrane holder (2.3-cm ID and 40.0 cm long). The holder was fitted with a high-pressure gas inlet and effluent outlet lines in the bore side of the membrane as well as with a low-pressure effluent outlet line in the permeate side. The feed-gas flow rate into the membrane at pressure  $P^H$  and the flow rates of both the high- and low-pressure effluent gases were measured using mass flowmeters (MFM). The low-pressure effluent gas was withdrawn in a direction countercurrent to that of the feed-gas flow. The feed-gas mixtures were premixed. The effluent-gas compositions were measured by a gas chromatograph (GC). A back-pressure regulator was used at the high-pressure effluent line to maintain a constant value of  $P^H$ . The low-pressure side of the membrane was maintained at a constant value of  $\sim 0.11$  MPa ( $= P^L$ ) for all tests. The system temperature was ambient ( $25 \pm 3^\circ\text{C}$ ). All effluent gases from the membrane were passed through an aqueous-alkali solution in order to remove the H<sub>2</sub>S before venting.

The experiments were conducted at a feed-gas pressure of 0.79 MPa using two different feed-gas mole fractions of H<sub>2</sub>S ( $y_{\text{H}_2\text{S}}^F = 0.25, 0.50$ ). The effluent gas flow rates and compositions were measured after steady-state operations were established, which typically took 0.5 h of operation.

The partial pressures of H<sub>2</sub>S and H<sub>2</sub> (both high- and low-pressure sides) vary along the length of the membrane under steady-state operation. Consequently, the amounts of H<sub>2</sub>S

and H<sub>2</sub> adsorbed on the membrane pore walls at both high- and low-pressure sides as well as their surface diffusivities vary along the membrane length. As a result, the H<sub>2</sub>S permeance and permselectivity are functions of the membrane length. These functionalities are not known. We therefore chose to describe the separation performance of the SSF membrane in terms of overall H<sub>2</sub> recovery ( $\alpha_{\text{H}_2}$ ) and H<sub>2</sub>S rejection ( $\beta_{\text{H}_2\text{S}}$ ). The H<sub>2</sub> recovery is defined by the ratio of the molar flow rates of H<sub>2</sub> in the high-pressure effluent gas stream to that in the feed-gas stream. The H<sub>2</sub>S rejection is defined by the ratio of the molar flow rates of H<sub>2</sub>S in the low-pressure effluent-gas stream to that in the feed-gas stream.

The separation performance data will be given in terms of  $\beta_{\text{H}_2\text{S}}$  as functions of  $\alpha_{\text{H}_2}$  for different feed-gas conditions. High rejections of H<sub>2</sub>S at high recoveries of H<sub>2</sub> are the desired properties. This mode of description of the separation performance of the SSF membrane also represents the practical separation characteristics by the membrane.

All gas flow rates and compositions for the membrane system can be expressed in terms of the variables  $\alpha_{\text{H}_2}$ ,  $\beta_{\text{H}_2\text{S}}$ , the feed-gas flow rate ( $F$ ), and  $y_{\text{H}_2}^F$  by carrying out mass balances.

### High-pressure-side effluent

$$\frac{P}{F} = \sum y_i^F (1 - \beta_i); \quad y_i^P = \frac{y_i^F (1 - \beta_i)}{\left[ \sum y_i^F (1 - \beta_i) \right]} \quad (1)$$

### Low-pressure-side effluent

$$\frac{W}{F} = 1 - \sum y_i^F (1 - \beta_i); \quad y_i^W = \frac{y_i^F \beta_i}{\left[ 1 - \sum y_i^F (1 - \beta_i) \right]}, \quad (2)$$

where  $P$  and  $y_i^P$  are, respectively, the molar flow rate and mole fraction of component  $i$  in the high-pressure effluent;  $W$  and  $y_i^W$  are the corresponding properties of the low-pressure effluent. It should be noted that ( $\alpha_i + \beta_i = 1$ ). The summations in Eqs. 1 and 2 are over both components ( $i = 1, 2$ ).

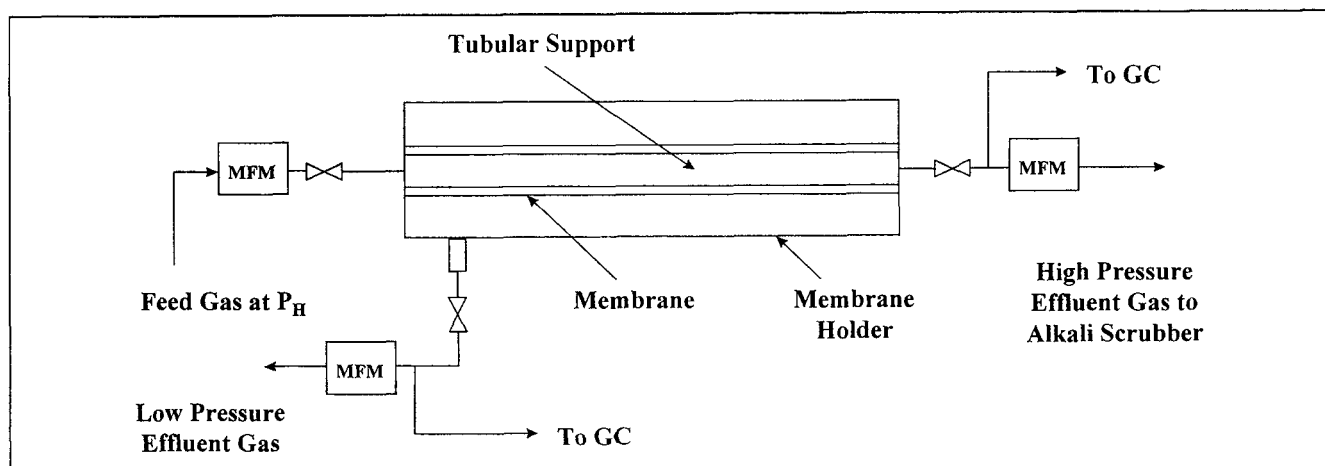


Figure 1. Experimental apparatus.

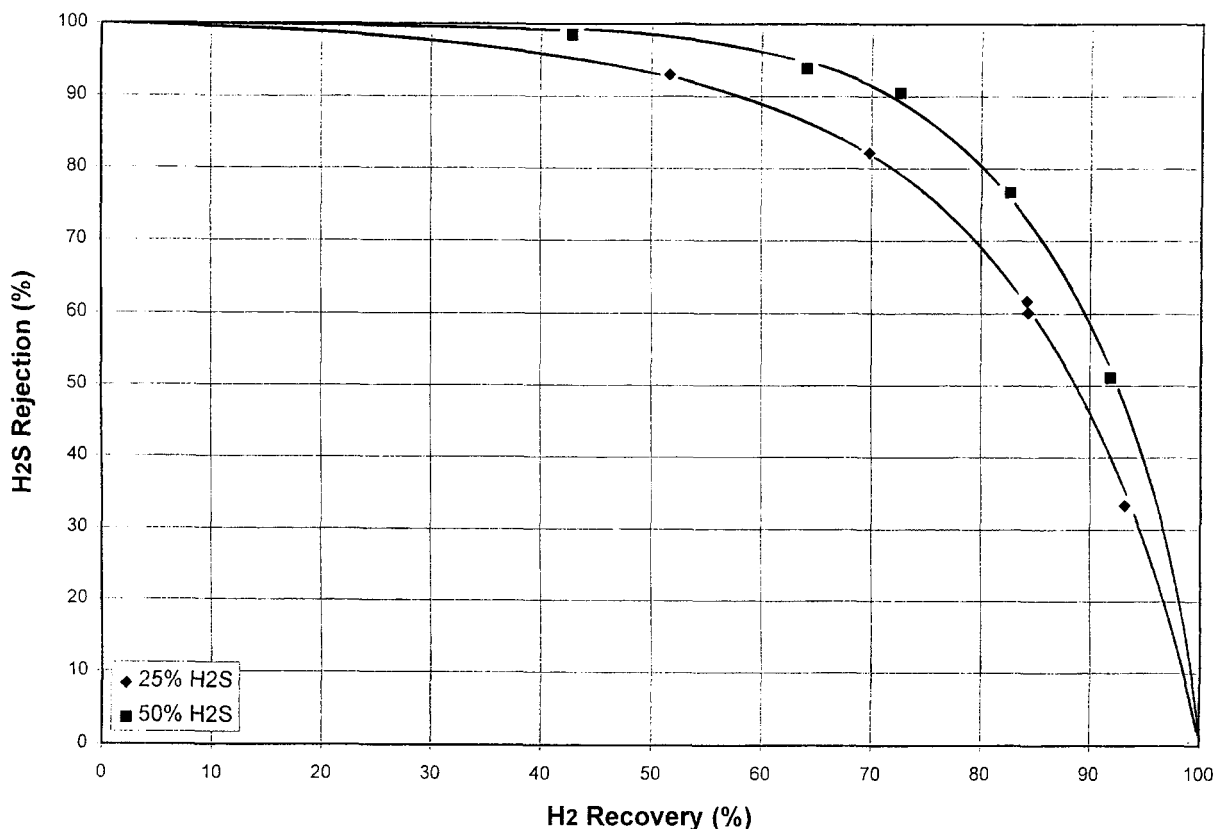


Figure 2. H<sub>2</sub>S rejection by the SSF membrane as functions of H<sub>2</sub> recovery.

## Experimental Results

Figure 2 shows the H<sub>2</sub>S rejection ( $\beta_{\text{H}_2\text{S}}$ ) against hydrogen recovery ( $\alpha_{\text{H}_2}$ ) plots measured in our laboratory. The feed-gas flow rate ( $F$ ) was varied at constant values of  $P^H$  and  $y_{\text{H}_2\text{S}}^F$  in order to generate these performance curves. The overall and component mass balances closed within  $\pm 3\%$  for each experimental run and the data were very reproducible. The curves of Figure 2 are bounded by the limits ( $\alpha_{\text{H}_2} = 0$ ,  $\beta_{\text{H}_2\text{S}} = 100$ ) and ( $\alpha_{\text{H}_2} = 100$ ,  $\beta_{\text{H}_2\text{S}} = 0$ ), and a straight line through these limiting points represents the case of no separation.

It may be seen from Figure 2 that H<sub>2</sub>S is preferentially permeated through the SSF membrane and the separation of bulk H<sub>2</sub>S from mixtures with H<sub>2</sub> improves as the partial pressure of H<sub>2</sub>S in the feed gas ( $p_{\text{H}_2\text{S}}^F$ ) is increased. An identical result was previously reported for separation of bulk CO<sub>2</sub>-H<sub>2</sub> mixture by the SSF membrane (Paranjape et al., 1997). Figure 2 also shows that a very high rejection of H<sub>2</sub>S at a high H<sub>2</sub> recovery can be achieved when the feed gas H<sub>2</sub>S mole fraction is large ( $y_{\text{H}_2\text{S}}^F \sim 0.5$ ). For example, the H<sub>2</sub>S rejections from a feed gas at 0.79 MPa containing 50% H<sub>2</sub>S are, respectively, 95+ % and 80% at H<sub>2</sub> recoveries of 60% and 80%. The H<sub>2</sub>S rejection can be increased to more than 98+ % if an H<sub>2</sub> recovery of less than 50% is acceptable. These figures demonstrate that the SSF membrane is very efficient for separation of bulk H<sub>2</sub>S-H<sub>2</sub> mixtures even at moderate feed-gas pressures.

## Empirical Data Representation

In absence of binary adsorption equilibrium and surface

diffusion data for the H<sub>2</sub>S-H<sub>2</sub> mixture on the SSF membrane, we empirically describe the rejection-recovery plots of Figure 2 by the following relationship:

$$\beta_{\text{H}_2\text{S}} = \frac{\psi(1 - \alpha_{\text{H}_2})}{1 + (\psi - 1)(1 - \alpha_{\text{H}_2})}, \quad (3)$$

where  $\psi$  is an empirical parameter. It is a function of the partial pressure of H<sub>2</sub>S ( $p_{\text{H}_2\text{S}}^F$ ) in the feed gas. The value of  $\psi$  is greater than unity for any separation to occur [ $\beta_{\text{H}_2\text{S}} + \alpha_{\text{H}_2} = 1$  for  $\psi = 1$ ]. The higher the value of  $\psi$ , the better the separation of H<sub>2</sub>S from H<sub>2</sub>. Equation 3 exhibits the appropriate boundary conditions for the rejection-recovery plots.

Figure 3 shows the fit of the rejection-recovery data of Figure 2 by Eq. 3. The values of  $\psi$  for different feed-gas mole fractions of H<sub>2</sub>S are given in the figure. Equation 3 describes the experimental data fairly well. Figure 4 shows that a linear empirical correlation exists between the variables  $\psi$  and  $p_{\text{H}_2\text{S}}^F$  over a large range of  $p_{\text{H}_2\text{S}}^F$  values. The line intersects the ordinate ( $p_{\text{H}_2\text{S}}^F = 0$ ) at a point where  $\psi$  is unity (as required). A linear correlation was also observed between the parameter  $\psi$  and the feed-gas partial pressures of CO<sub>2</sub>. ( $p_{\text{CO}_2}^F$ ) for separation of binary CO<sub>2</sub>-H<sub>2</sub> mixtures by the SSF membrane (Paranjape et al., 1997). A much larger database was available for that case. The dashed line in Figure 4 shows the  $\psi - (p_{\text{CO}_2}^F)$  plot for comparison. It may be seen that the slope of the  $\psi - p_{\text{H}_2\text{S}}^F$  plot is about three times larger than the slope of the corresponding plot for CO<sub>2</sub>-H<sub>2</sub> separation. Thus, the SSF membrane is more efficient for the separation

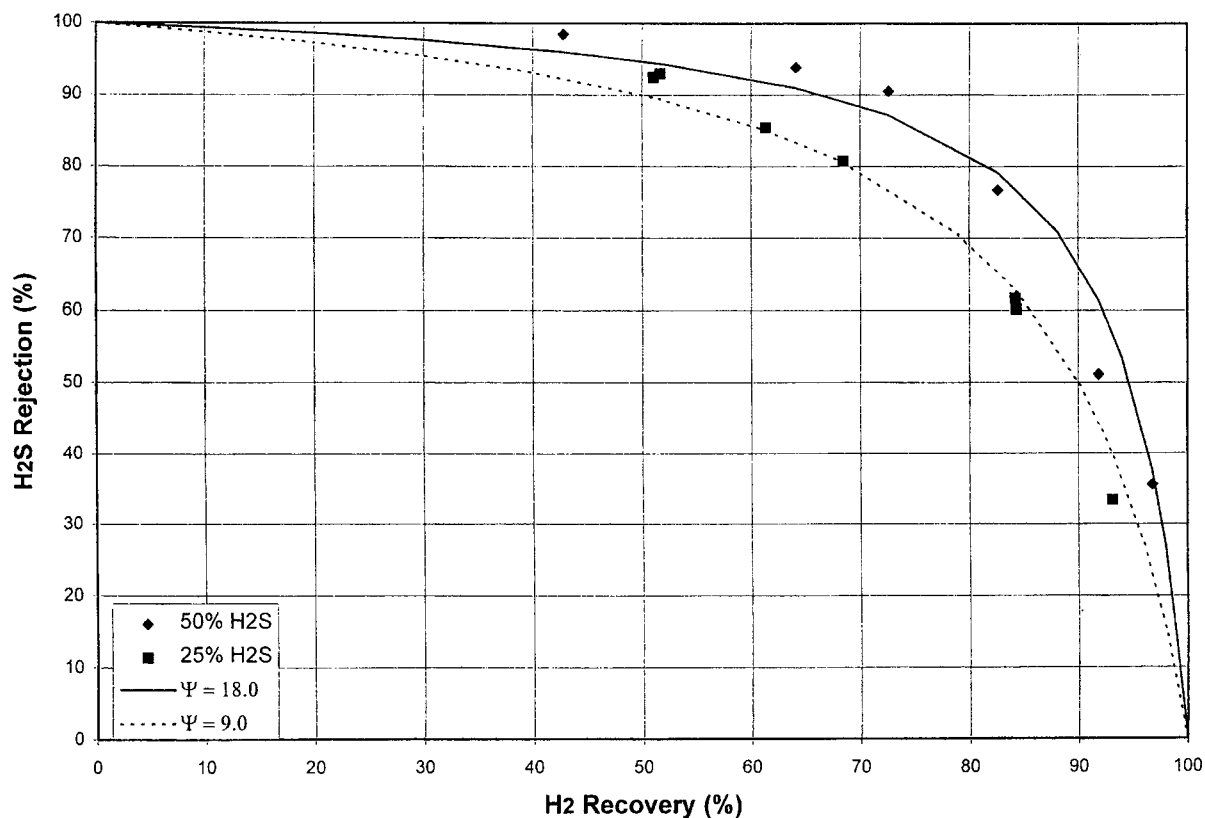


Figure 3. Fit of data of Figure 2 by Eq. 3.

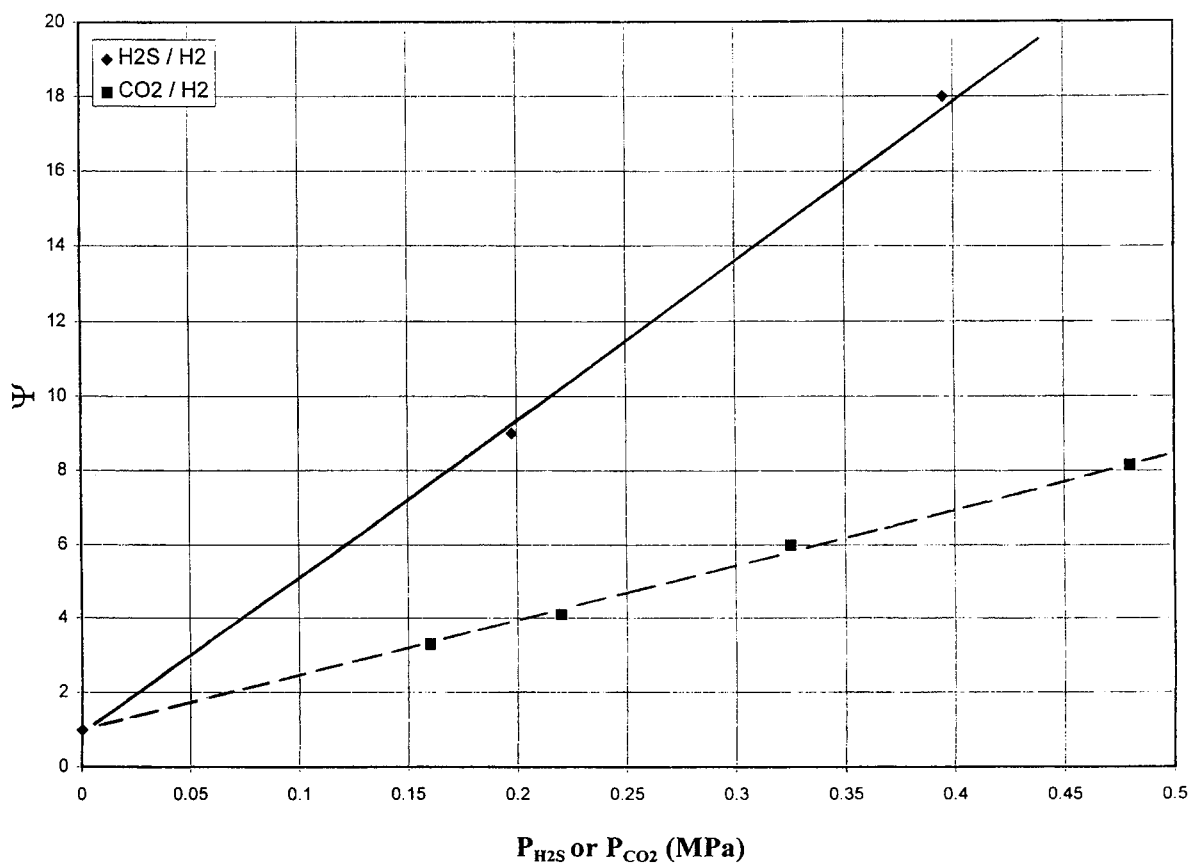


Figure 4. Dependence of empirical parameter ( $\psi$ ) on feed-gas partial pressures of H<sub>2</sub>S ( $p_{\text{H}_2\text{S}}^F$ ) or CO<sub>2</sub> ( $p_{\text{CO}_2}^F$ ).

of bulk  $\text{H}_2\text{S}$ - $\text{H}_2$  mixtures than that for  $\text{CO}_2$ - $\text{H}_2$  mixtures. This is caused by the larger affinity of adsorption of  $\text{H}_2\text{S}$  on the nanoporous carbon walls than  $\text{CO}_2$ .

### Novel Mode of Operation of SSF Membrane

The separation goal is to produce a highly enriched stream of  $\text{H}_2$  at feed-gas pressure with high  $\text{H}_2$  recovery from a bulk  $\text{H}_2\text{S}$ - $\text{H}_2$  mixture by selectively rejecting  $\text{H}_2\text{S}$  through the SSF membrane. We found that a two-stage embodiment of the SSF membrane described by Figure 5 can achieve that goal when it is operated using a specific protocol (Sircar and Parillo, 1997).

The feed gas is introduced into the high-pressure side of the stage 1 of the membrane assembly at pressure  $P^{H1}$  and a  $\text{H}_2$ -enriched product gas is withdrawn from that membrane at essentially the feed-gas pressure. The  $\text{H}_2\text{S}$ -enriched permeated gas is withdrawn countercurrently from the low-pressure side of the stage 1 membrane at pressure  $P^L$ . It is then compressed to a pressure level of  $P^{H2}$  ( $\leq P^{H1}$ ) and introduced into the feed side of stage 2 of the membrane assembly. The high-pressure effluent gas from the stage 2 membrane is recompressed to  $P^{H1}$  and reintroduced as feed gas to the stage 1 membrane by mixing it with the fresh feed gas. The low-pressure effluent from stage 2 membrane at pressure  $P^L$  is countercurrently withdrawn as the  $\text{H}_2\text{S}$  enriched product gas. Neither stage uses any purge gas at the low-pressure side. This configuration of a two-stage membrane is well known (Spillman, 1989). However, it will be demonstrated later that a specific mode of operation of the two-stage membrane can simultaneously provide high recovery and purity of the  $\text{H}_2$  product.

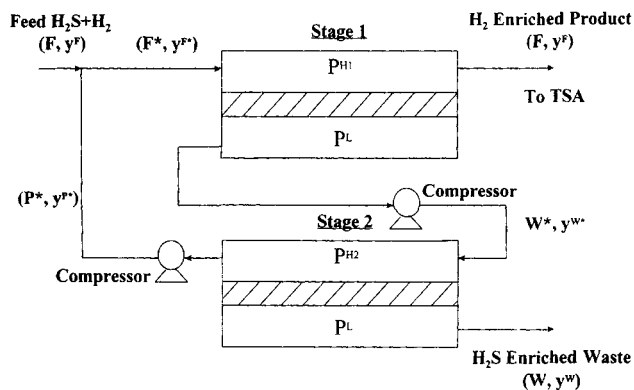


**Figure 5. Flowsheet for two-stage operation of the SSF membrane.**

The variables  $F$ ,  $F^*$ ,  $P$ ,  $W^*$ ,  $P^*$ , and  $W$  represent the molar flow rates of various streams entering and leaving the two stages of the membrane assembly as depicted by Figure 5. The variables  $y^F$ ,  $y^{F^*}$ ,  $y^P$ ,  $y^{W^*}$ ,  $y^{P^*}$ , and  $y^W$  represent the mole fractions of  $\text{H}_2\text{S}$  in the corresponding streams. We designate the  $\text{H}_2$  recoveries of membrane stages 1 and 2 by the variables  $\alpha_1$  and  $\alpha_2$ , respectively, and the  $\text{H}_2\text{S}$  rejections of the membrane stages 1 and 2 by the variables  $\beta_1$  and  $\beta_2$ , respectively. Equations 1 and 2 can then be combined with appropriate mass-balance equations for the membrane stages to obtain analytical expressions describing the flow rate and composition of each stream of Figure 5 in terms of feed-gas flow rate ( $F$ ), the feed-gas composition ( $y^F$ ) and the variables  $\alpha_1$ ,  $\alpha_2$ ,  $\beta_1$ , and  $\beta_2$ . They are summarized below.

#### Flow rates

$$F^* = \frac{F[1 - (1 - \alpha_1)\alpha_2 y^F - \beta_1(1 - \beta_2)(1 - y^F)]}{[1 - \beta_1(1 - \beta_2)][1 - \alpha_2(1 - \alpha_1)]}$$

$$P^* = \frac{F[\beta_1(1 - \beta_2)\{1 - \alpha_2(1 - \alpha_1)\}y^F + \alpha_2(1 - \alpha_1)\{1 - \beta_1(1 - \beta_2)\}(1 - y^F)]}{[1 - \beta_1(1 - \beta_2)][1 - \alpha_2(1 - \alpha_1)]}$$

$$W^* = \frac{F[1 - \{1 - \beta_1[1 - \alpha_2(1 - \alpha_1)]\}y^F - \{\alpha_1 + \beta_1(1 - \beta_2)(1 - \alpha_1)\}(1 - y^F)]}{[1 - \beta_1(1 - \beta_2)][1 - \alpha_2(1 - \alpha_1)]}$$

$$P = \frac{F[(1 - \beta_1)\{1 - \alpha_2(1 - \alpha_1)\}y^F + \alpha_1\{1 - \beta_1(1 - \beta_2)\}(1 - y^F)]}{[1 - \beta_1(1 - \beta_2)][1 - \alpha_2(1 - \alpha_1)]}$$

$$W = \frac{F[1 - \{1 - \beta_1\beta_2[1 - \alpha_2(1 - \alpha_1)]\}y^F - \{\beta_1(1 - \beta_2) + [1 - \beta_1(1 - \beta_2)][\alpha_1 + \alpha_2 - \alpha_1\alpha_2]\}(1 - y^F)]}{[1 - \beta_1(1 - \beta_2)][1 - \alpha_2(1 - \alpha_1)]}$$

#### Compositions

$$y^{F^*} = \frac{y^F[1 - (1 - \alpha_1)\alpha_2]}{[1 - (1 - \alpha_1)\alpha_2 y^F - \beta_1(1 - \beta_2)(1 - y^F)]}$$

$$y^{P^*} = \frac{y^F[1 - \alpha_2(1 - \alpha_1)][\beta_1(1 - \beta_2)]}{[\beta_1(1 - \beta_2)\{1 - \alpha_2(1 - \alpha_1)\}y^F + \alpha_2(1 - \alpha_1)\{1 - \beta_1(1 - \beta_2)\}(1 - y^F)]}$$

$$y^{W*} = \frac{y^F(\beta_1)[1 - \alpha_2(1 - \alpha_1)]}{[1 - \{1 - \beta_1[1 - \alpha_2(1 - \alpha_1)]\}y^F - \{\alpha_1 + \beta_1(1 - \beta_2)(1 - \alpha_1)\}(1 - y^F)]}$$

$$y^P = \frac{y^F(1 - \beta_1)[1 - \alpha_2(1 - \alpha_1)]}{[(1 - \beta_1)\{1 + \alpha_2(1 - \alpha_1)\}y^F + \alpha_1\{1 - \beta_1(1 - \beta_2)\}(1 - y^F)]}$$

$$y^{W*} = \frac{y^F\beta_1\beta_2[1 - \alpha_2(1 - \alpha_1)]}{[1 - \{1 - \beta_1\beta_2[1 - \alpha_2(1 - \alpha_1)]\}y^F - \{\beta_1(1 - \beta_2) + [1 - \beta_1(1 - \beta_2)][\alpha_1 + \alpha_2 - \alpha_1\alpha_2]\}(1 - y^F)]}$$

It can also be shown that the overall H<sub>2</sub> recovery [ $\alpha = P(1 - y^P)/F(1 - y^F)$ ] and H<sub>2</sub>S rejection [ $\beta = Wy^W/Fy^F$ ] by the membrane assembly of Figure 5 are given by:

$$\alpha = \frac{\alpha_1}{1 - (1 - \alpha_1)\alpha_2} \quad (4)$$

$$\beta = \frac{\beta_1\beta_2}{1 - \beta_1(1 - \beta_2)} \quad (5)$$

By choosing a set of values for the variables  $F$ ,  $y^F$ ,  $\alpha_1$ ,  $\alpha_2$ ,  $P^{H1}$ , and  $P^{H2}$ , and by guessing the values of parameters of  $y^{F*}$  ( $< y^F$ ) and  $y^{W*}$  ( $> y^F$ ), one can estimate the values of parameters  $\psi_1$ ,  $\psi_2$ ,  $\beta_1$ , and  $\beta_2$  by using Eq. 3 and Figure 4. The analytical equations just listed can then be used to calculate  $y^{F*}$  and  $y^{W*}$ , and the process repeated until convergence between the chosen and calculated values of these two variables is obtained. The converged values of  $\psi_1$ ,  $\psi_2$ ,  $\beta_1$ , and  $\beta_2$  can then be used to calculate the flow rates and compositions of all streams as well as the overall H<sub>2</sub> recovery (Eq. 4) and the overall H<sub>2</sub>S rejection (Eq. 5) by the membrane system. Alternatively, the two-stage membrane can be operated using constant partial pressures ( $p_{H_2S}^F$ ) of H<sub>2</sub>S in the feed gas for both stages ( $F^*$  and  $W^*$ ). Thus, ( $\psi_1 = \psi$ ), and a single rejection–recovery curve (Figure 2) determines  $\beta_{H_2S}$  as functions of  $\alpha_{H_2}$  for both stages. One can then choose values of the parameters,  $F$ ,  $y^F$ ,  $\alpha_1$ , and  $\alpha_2$  and calculate the flow rates and compositions of all streams of Figure 5 as well as  $\alpha$  and  $\beta$ , using the equations just listed and Eqs. 4 and 5. The operating pressures ( $P^{H1}$  and  $P^{H2}$ ) of the two stages of the membrane can then be easily calculated from  $p_{H_2S}^F$ ,  $y^{F*}$ , and  $y^{W*}$  values.

We used the second approach to estimate the performance of the two-stage membrane embodiment of Figure 5 for separation of an equimolar H<sub>2</sub>S–H<sub>2</sub> feed-gas mixture ( $y^F = 0.5$ ). Different combinations of  $\alpha_1$  and  $\alpha_2$  values were chosen. A feed gas H<sub>2</sub>S partial pressure of 0.395 MPa (curve of Figure

2) was chosen for both stages of the membrane. The results are shown in Table 1.

It may be clearly seen from Table 1 that the desired separation goal can be achieved by operating the two-stage membrane embodiment of Figure 5 using a low recovery of H<sub>2</sub> for stage 1 membrane and a high recovery of H<sub>2</sub> for stage 2 membrane ( $\alpha_1 < \alpha_2$ ). For example, using the values of 0.3 and 0.9 for the variables  $\alpha_1$  and  $\alpha_2$ , respectively, this novel protocol for operation of the membrane system can yield an ~98% pure H<sub>2</sub> product stream at 81% H<sub>2</sub> recovery. The product is obtained at the feed-gas pressure (~1.01 MPa). About 98% of feed H<sub>2</sub>S is rejected by the membrane system and the H<sub>2</sub>S-enriched effluent gas contains 83.8% H<sub>2</sub>S. It is produced at near-ambient pressure. Increasing the ratio of ( $\alpha_1/\alpha_2$ ) significantly lowers the H<sub>2</sub> product purity or its recovery.

One major advantage of directly producing a high-purity H<sub>2</sub> product ( $y_{H_2}^P > 97\%$ ) by the membrane system is that it can be further purified to an essentially pure H<sub>2</sub> ( $y_{H_2} = 99.99 + \%$ ) product stream at feed gas pressure by removing the dilute H<sub>2</sub>S impurity in a conventional thermal-swing adsorption (TSA) process. The typical H<sub>2</sub> loss in a TSA purification system is only between 5 and 10%. On the other hand, if the H<sub>2</sub> enriched product gas from the membrane system contains more than 3% H<sub>2</sub>S, a pressure-swing adsorption (PSA) process will be needed to produce a pure H<sub>2</sub> product. The typical H<sub>2</sub> loss in a PSA purification system is typically between 20 and 30%. Thus, the novel mode of operation of the two-stage membrane described earlier allows higher overall recovery of pure H<sub>2</sub> from a bulk H<sub>2</sub>S–H<sub>2</sub> mixture by the use of a hybrid membrane–TSA separation device.

## Summary

The SSF membrane can be efficiently used to separate bulk H<sub>2</sub>S–H<sub>2</sub> mixtures. H<sub>2</sub>S is selectively permeated through the membrane. The H<sub>2</sub>S rejection–H<sub>2</sub> recovery characteristics of

**Table 1. Performance of Two-stage SSF Membrane for Bulk H<sub>2</sub>S–H<sub>2</sub> Separation (Equimolar Feed Gas)**

Stage H <sub>2</sub> Recoveries			H <sub>2</sub> -Enriched Product Gas		H <sub>2</sub> S-Enriched Reject Gas		Operating Pressures	
$\alpha_1$	$\alpha_2$	( $\alpha_1/\alpha_2$ )	H <sub>2</sub> Purity (mol %)	Recovery ( $\alpha$ %)	H <sub>2</sub> S Purity (mol %)	Rejection ( $\beta$ %)	pH1 (MPa)	pH2 (MPa)
0.30	0.90	0.33	97.9	81.0	83.8	98.3	1.00	0.83
0.30	0.60	0.50	98.0	51.7	67.2	98.9	1.06	0.86
0.30	0.30	1.00	97.4	38.0	61.5	99.0	0.89	0.74
0.60	0.30	2.00	95.7	68.1	75.2	97.0	0.84	0.58
0.75	0.30	2.50	87.1	81.0	82.2	87.8	0.82	0.52
0.90	0.30	3.00	68.2	92.7	88.6	56.7	0.80	0.47

the membrane can be described by a single-parameter empirical model.

A two-stage embodiment of the SSF membrane can be operated to produce a high-purity  $H_2$  product (mole fraction  $\sim 98.0\%$ ) with high  $H_2$  recovery ( $\sim 80\%$ ) at the feed-gas pressure from an equimolar  $H_2S-H_2$  feed gas. This can be achieved by a novel protocol of operation of the membrane where the  $H_2$  recoveries of the two membrane stages are controlled in a specific manner.

## Acknowledgment

This work was partly supported by the U.S. Department of Energy, Assistant Secretary for Energy Efficiency and Renewable Energy, Office of Industrial Technologies, under DOE Albuquerque Operations Office Co-operative Agreement DE FC 04-94 AL 94461. The authors are grateful to Mr. P. Novosat for carrying out the experimental work.

## Notation

- $F^*$  = total feed-gas flow rate to stage 1 of membrane system of Figure 5  
 $P^*$  = flow rate of high-pressure recycle gas in membrane system of Figure 5  
 $W^*$  = flow rate of feed gas to stage 2 of membrane system of Figure 5

## Subscripts and superscripts

- 1, 2 = stages 1 and 2 of membrane of Figure 5

## Literature Cited

- Anand, M., M. B. Rao, and S. Sircar, "Hydrogen Recovery by Adsorbent Membranes," U.S. Patent No. 5,435,836 (1995).  
Anand, M., M. Langsam, M. B. Rao, and S. Sircar, "Multicomponent Gas Separation by SSF and PTMSP Membranes," *J. Memb. Sci.*, **123**, 17 (1997).  
Breck, D. W., *Zeolite Molecular Sieves: Structure, Chemistry and Use*, Wiley, New York (1973).  
Hirschfelder, J. O., C. F. Curtis, and R. B. Bird, *Molecular Theory of Gases and Liquids*, Wiley, New York (1954).  
Paranjape, M., P. F. Clarke, B. B. Pruden, D. J. Parrillo, C. Tharon, and S. Sircar, "Separation of Bulk  $CO_2-H_2$  Mixtures by Selective Surface Flow Membranes," *Can. J. Chem. Eng.*, in press (1997).  
Rao, M. B., S. Sircar, and T. C. Golden, "Gas Separation by Adsorbent Membranes," U.S. Patent No. 5,104,425 (1992).  
Rao, M. B., and S. Sircar, "Nanoporous Carbon Membranes for Separation of Gas Mixtures by Selective Surface Flow," *J. Memb. Sci.*, **85**, 253 (1993).  
Rao, M. B., and S. Sircar, "Performance and Pore Characterization of Nanoporous Carbon Membranes for Gas Separation," *J. Memb. Sci.*, **110**, 109 (1996).  
Rao, M. B., S. Sircar, J. M. Abrardo, and W. F. Baade, "Hydrogen Recovery by Adsorbent Membranes," U.S. Patent No. 5,447,559 (1995).  
Sircar, S., and D. J. Parrillo, "Operation of SSF Membrane for Enhanced Separation Efficiency," U.S. Patent No. (1997), pending.  
Spillman, R. W., "Economics of Gas Separation," *Chem. Eng. Prog.*, **85**(1), 41 (1989).  
Stogryn, D. E., and A. P. Stogryn, "Molecular Multipole Moments," *Mol. Phys.*, **11**, 371 (1966).  
Weast, R. C., and M. J. Astle, eds., *CRC Handbook of Chemistry and Physics*, 59th ed., CRC Press, West Palm Beach, FL (1974).

Manuscript received Jan. 27, 1997, and revision received Apr. 11, 1997.